

Assessment of Effects of Neutrals on the Power Threshold for L to H Transitions in DIII-D

L W Owen[†], B A Carreras[†], R Maingi[†], P K Mioduszewski[†], T N Carlstrom[†] and R J Groebner[‡]

[†]Oak Ridge National Laboratory, Oak Ridge, Tennessee 37831

[‡]General Atomics, San Diego, California 92186-9784

CONF-980915--
RECEIVED
AUG 11 1998
OSTI

Abstract. To assess the effect of edge neutrals on the low-to-high confinement transition threshold, a broad range of plasma discharges has been analyzed. From this analysis, the transition power divided by the density, at constant magnetic field, appears to be a function of a single parameter measuring the neutrals' effect. This results suggest that there is a missing parameter linked to the neutrals in the power threshold scaling laws.

1. Introduction

One of the characteristic properties of the transition from the low confinement mode (L-mode) to the high confinement mode (H-mode) [1], [2] is a power threshold. From the early experiments, the power threshold, P_{th} , generally increases with line-averaged electron density, \bar{n} , and magnetic field, B [3]-[5]. A scaling law of the form $P_{th} \propto \bar{n}B$ was proposed [6]. This scaling is found for single null divertor configurations with the ∇B direction towards the X-point. A power-threshold database exists from several devices operating in conditions similar to those of the present International Thermonuclear Experimental Reactor (ITER) design. These data permit the refinement of this scaling law, and variants have been obtained by requiring dimensionally correct parametric dependences and by including the device size dependence [7],[8]. However, there is not yet a scaling law that describes the data well enough to allow an extrapolation to ITER conditions with reasonable certainty. Evidence for the importance of atomic physics effects surfaced in the first experiments that showed that access to the H-mode requires careful wall conditioning and a reduction in the wall recycling [9]. It is also well known that changes in wall conditioning and configuration can cause significant changes in the power threshold [10]. However, there is very little information on how wall conditioning affects the low to high L-to-H transition. An obvious potential mechanism is the coupling of the neutral dynamics to the transition mechanism, as indicated in several experiments [11]-[14]. Theoretical models have included the effect of neutrals on the L-to-H transition dynamics [15]-[19]. A principal mechanism is the change of the ion momentum balance through charge exchange friction.

2. Analysis of the gas puff, pumping, and density scan experiments

The data used in this analysis is a subset of discharges from two power threshold experiments performed in DIII-D as part of the ITER physics studies [8]. All these discharges are lower single-null divertor discharges with the shaping parameters similar to the ITER shape. The ion ∇B drift is toward the X-point and the toroidal field is 2.1T.

MASTER
JAT

DISCLAIMER

This report was prepared as an account of work sponsored by an agency of the United States Government. Neither the United States Government nor any agency thereof, nor any of their employees, make any warranty, express or implied, or assumes any legal liability or responsibility for the accuracy, completeness, or usefulness of any information, apparatus, product, or process disclosed, or represents that its use would not infringe privately owned rights. Reference herein to any specific commercial product, process, or service by trade name, trademark, manufacturer, or otherwise does not necessarily constitute or imply its endorsement, recommendation, or favoring by the United States Government or any agency thereof. The views and opinions of authors expressed herein do not necessarily state or reflect those of the United States Government or any agency thereof.

DISCLAIMER

Portions of this document may be illegible in electronic image products. Images are produced from the best available original document.

The first experiment, performed in 1994, is a power threshold density scan [22]. The density dependence of the power threshold, defined as the power through the separatrix, at the moment of the transition [21], showed the characteristic shallow U-shape observed in several devices. The second experiment was a series of discharges carried out in 1996 to test the neutrals' effects on the power threshold [20] with active control of the neutrals. Three variants were tried with the intention of changing the neutral density without changing the plasma parameters too much: 1) a strong gas puff from the top of the machine to increase the ratio of neutral to electron density; 2) the cryopump on, with the goal of decreasing the neutral density; and 3) the X-point moved closer to the target plate. The power threshold for the discharges with the cryopump on is 70% larger than that for the gas puff discharges, and the densities are about 20% to 40% lower. The results of this experiment were counter-intuitive in the sense that the discharges for which the goal was to increase the neutral density had lower power threshold than the ones for which the goal was to decrease it.

The analysis of the data involves two steps. Since the neutral density distribution at the plasma edge is not measured, we must first reconstruct the neutral density and temperature distributions and the corresponding plasma-neutral reaction rates. This is done by fitting the measured plasma parameters with the B2.5 edge plasma transport code [23] and generating the neutrals profiles with the DEGAS code [24]. These codes are used iteratively but not coupled. Details of the analysis are given in Ref. 21. The second part of the analysis is the evaluation of parameters that may characterize the role of neutrals in the L-to-H transition, such as the charge exchange damping rate, ν_{CX} , and the neoclassical poloidal flow damping rate, μ_{neo} .

The calculated density profiles of neutrals in the SOL show that the neutral density responded as expected in the experiment. That is, the discharges with added gas puff and lower X-point have larger neutral density in the SOL than the standard case and the discharges with the cryopump on have lower SOL neutral density. The neutral density response inside the separatrix is the opposite to what it is in the SOL. The gas puff and lower X-point discharges have lower neutral density than the standard discharge, while discharges with the cryopump on have higher neutral density. This behavior of the neutrals is caused by the nonlinear character of the fueling dynamics. When gas is puffed, the neutral density in the SOL increases, causing an increase in the particle source. Because of the enhancement in the particle source, the plasma edge density increases. The neutral ionization mean free path is inversely proportional to plasma density, so the neutral particle decay length inside the separatrix becomes shorter. The resulting profiles are such that the neutral density is larger in the SOL and smaller inside the separatrix than those for the standard discharge. In spite of the reduction of neutral density inside the separatrix the particle source remains larger for the gas puff discharges than for the standard discharge. Also the lower edge neutral density around the X-point results in a decrease of approximately a factor of five in the maximum charge exchange damping rate with gas puffing when compared to the standard discharge.

With lower X-point the neutral density close to the X-point and the particle source are larger when compared with the standard discharge. The edge temperature is 20% lower and

the power input at the transition is higher in the standard discharge. These discharges with a lower X-point have an enhanced particle source term, with properties similar to a discharge with a very mild gas puff. Therefore, the argument from the case of gas puff discharges carries over to this case. The discussion of the gas puff discharges can be applied in reverse to the discharges with the cryopump on. For the pumped discharges, which have the highest power threshold, the charge exchange damping dominates the neoclassical damping near the X-point region. This suggests that neutrals are playing an important role.

For the 1994 density scan experiments, the two factors discussed above again play a role in determining the neutral density inside the separatrix: (1) the particle source term which increases as the line-averaged density increases, and (2) the neutral density penetration length, that decreases with increasing line-averaged density. Since the neutral profiles decay toward the inside of the plasma in a quasi-exponential fashion, the reduction in decay length quickly becomes the dominant factor. Therefore, inside of the separatrix region the low density plasma has higher neutral density than the high density plasmas.

3. Discussion and Conclusions

For averaged radius in the region $0.9 > r/r_S > 0.95$, we have found good correlation of P_{sep}/\bar{n} with either the charge-exchange damping rate or the neutral density. It is useful to consider dimensionless parameters representing the effect of neutrals. Since a mechanism possibly responsible for the neutrals' effect on the transition threshold is a change in the damping of the poloidal component of the $E \times B$ shear flow, we consider the parameter $(v_{CX})_M/\mu_{neo}$. Here $(v_{CX})_M$ is the maximum value of the charge exchange damping rate on a fixed flux surface. In Figure 1, we have plotted P_{sep}/\bar{n} as a function of $(v_{CX})_M/\mu_{neo}$ for the $r/r_S = 0.95$ surface. The correlation is very good considering the scattering of the initial data. A fit to the data gives $P_{sep} = \bar{n} \left[0.37 + 0.63 (v_{CX})_M^2 / \mu_{neo}^2 \right]$. Here, we express power in MW, and density in units of 10^{20} m^{-3} . Since $(v_{CX})_M/\mu_{neo}$ increases (decreases) with decreasing (increasing) line-averaged density, the combination of \bar{n} increasing and $(v_{CX})_M/\mu_{neo}$ decreasing gives a U-shape dependence for P_{sep} as a function of \bar{n} . This dependence is similar to the one observed in the threshold density scan experiments.

A good correlation is also obtained between P_{sep}/\bar{n} and λ_n/r_S , where, λ_n is the poloidally averaged neutral profile radial decay length (from the separatrix inwards), but such a fit gives a weak U-shape dependence of the power threshold on density. Other parametric dependences are possible. However, having studied experiments from only a single device, it is not possible to discriminate among these possible parameters.

Among other possible correlations between local plasma edge and neutrals parameters, these data also show a correlation between v_i^* and n_0/n_e at $r/r_S = 0.95$, as also seen in JT-60U [13], [14]. As can be expected, v_i^* also correlates well with $(v_{CX})_M/\mu_{neo}$. This correlation may be consistent with the change of the $v_i^* = \text{constant}$ threshold criterion [25] when modified by the neutral effects [16].

Acknowledgments

We gratefully acknowledge A. Mahdavi on the experimental planning of the gas puff and pumping experiments, S. H. Hirshman and D. J. Sigmar for useful discussions on the calculation of neoclassical

viscous force, M. Rensink and B. Braams for allowing us to use their numerical tools, and K. H. Burrell, P. H. Diamond, and M. Wade for multiple discussions of neutrals effects. Research sponsored by the Office of Fusion Energy, U.S. Department of Energy, under contract DE-AC05-96OR22464 with Lockheed Martin Energy Research Corp and DE-AC03-89ER51114 with General Atomics.

References

- [1] Wagner F, Becker G, Behringer K *et al.* 1982 *Phys. Rev. Lett.* **49** 1408
- [2] Burrell K H 1994 *Plasma Phys. and Control. Fusion* **36**, A291 (1994)
- [3] Burrell K H, Allen S L, Bramson G *et al.* 1988 *Proc. 12th Int. Conf. on Plasma Physics and Controlled Nuclear Fusion Research* vol 1 (Vienna: IAEA) p 193
- [4] Tanga A, Bartlett D, Bures M *et al.* 1988 *Proc. 15th EPS Conf. on Controlled Fusion and Plasma Heating*, ed EPS, vol. 12B Part 1 (Dubrovnik: EPS) p 235
- [5] Ryter F, Stroth U, Wagner F *et al.* 1992 *Proc. 19th EPS Conf. on Controlled Fusion and Plasma Physics* ed K L W Freysinger, R Schrittwieser, W Lindinger, vol 16C, Part I (Innsbruck: EPS), p. 1195
- [6] Kardaun O, Ryter F, Stroth U *et al.* 1992 *Proc. 14th Int. Conf. on Plasma Physics and Controlled Nuclear Fusion Research*, vol 3, (Vienna: IAEA) p 251
- [7] Ryter F and H mode database working group 1996 *Nucl. Fusion* **36** 1217
- [8] Takizuka T, Boucher D, Bracco G *et al.* 1996 *16th IAEA Fusion Energy Conf.* (Vienna: IAEA)
- [9] ASDEX Team 1989 *Nucl. Fusion* **29** 1959
- [10] Carlstrom T N, Gohil P, Watkins J G *et al.* 1994 *Plasma Phys. Control. Fusion* **36** A147
- [11] Mahdavi M A, Brooks N, Buchenauer D *et al.* 1990 *J. Nucl. Materials* **176&177** 32
- [12] Shimada M and JT-60 Team, 1992 in *Proc. 14th Int. Conf. on Plasma Physics and Controlled Nuclear Fusion Research* vol. 1 (Vienna: IAEA) p. 57
- [13] Tsuchiya K, Takenaga H, Fukuda T *et al.* 1996 *Plasma Phys. Control. Fusion* **38** 1295
- [14] Fukuda T, Sato M, Takizuka T *et al.* 1996 *Sixteenth IAEA Fusion Energy Conference* (Vienna: IAEA)
- [15] Shaing K C 1993 *Phys. Fluids B* **5** 3841
- [16] Shaing K C and Hsu C T 1995 *Phys. Plasmas* **2** 1801
- [17] Carreras B A, Diamond P H, and Vetoulis G 1996 *Phys. Plasmas* **3** 4106
- [18] Toda S, Itoh S-I, Yagi M *et al.* 1997 *Plasma Phys. Control. Fusion* **39** 301
- [19] Leonov V M and Polevoj A R 1994 *Proc. 15th Int. Conf. on Plasma Physics and Controlled Nuclear Fusion Research* vol 3 (Vienna: IAEA) p. 315
- [20] Groebner R J, Carlstrom T S, Burrell K H *et al.* 1996 *16th IAEA Fusion Energy Conf.* (Vienna: IAEA).
- [21] Carreras B A, Owen L W, Maingi R *et al.* 1997 *Phys. Plasmas*
- [22] Carlstrom T N and Groebner R J 1996 *Phys. Plasmas* **3** 1867.
- [23] Braams B J 1996 *Contrib. Plasma Phys.* **36** 276
- [24] Heifetz D B, Post D, Petravic M *et al.* 1982 *J. Comp. Phys.* **46** 309
- [25] Shaing K C, Crume J E C, and Houlberg W A 1988 *Comments Plasma Physics and Controlled Fusion* **12** 69

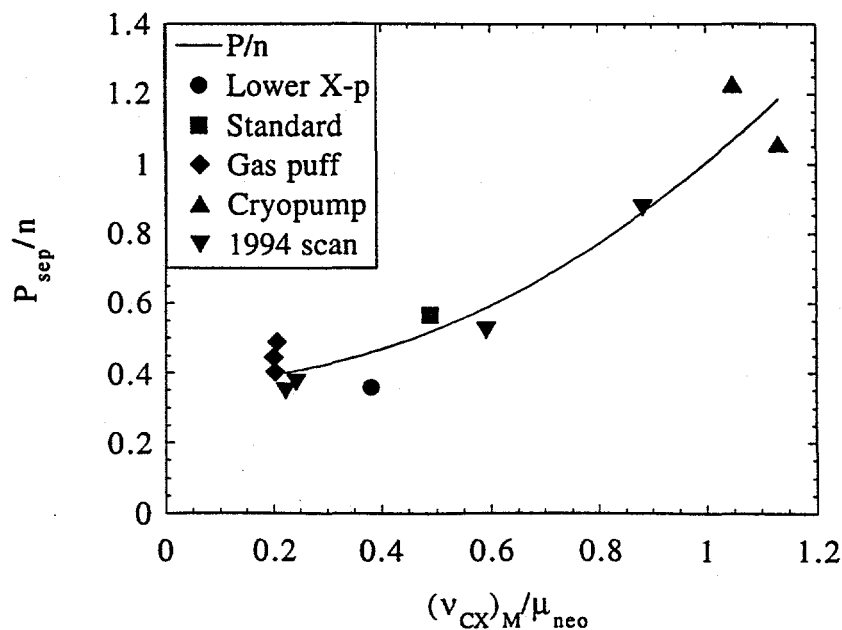


Figure 1. P_{sep}/\bar{n} as a function of $(v_{CX})_M/\mu_{neo}$ for the $r/a = 0.95$ surface.